Comparative Evaluation of Four RANS Turbulence Models for Aerosol Dispersion from a Cough

Jibola Owolabi[1] , *Khawaja Hassan*[1], and *Amar Aganovic* [1]
[1] Institute of Automation and Process Engineering (IAP), Faculty of Engineering Science and Technology (IVT), UiT, The Arctic University Norway, Tromsø, Norway.

Abstract. The study of aerosol dispersion in indoor environments is essential to understanding and mitigating airborne virus transmission, such as SARS-CoV-2. Computational Fluid Dynamics (CFD) has emerged as a valuable tool for investigating aerosol dispersion, providing an alternative to costly experimental methods. In this study, we investigated the performance of four (4) Reynolds-averaged Navier-Stokes (RANS) turbulence models in predicting aerosol dispersion from a human body coughing in a small, ventilated indoor environment. We compared the Standard, RNG, Realizable k-ϵ models and the SST k- ω model using the same boundary conditions. We initially observed that the horizontal distance of the coughed aerosols after 10.2s dispersion time was substantially shorter with the standard k-ϵ turbulence compared to the other three turbulence models compared to the SST k-ω model, the RNG, and realizable k-ϵ models exhibit a high degree of similarity in their dispersion patterns. Specifically, we observed that the aerosols dispersed horizontally faster with the RNG and Realizable k-ϵ models. In conclusion, when compared to qualitative data from the literature, our observations exclude the standard k-ϵ turbulence. However, to select the most appropriate turbulence model for capturing the cough flow and aerosol dispersion dynamics, further detailed validation against both quantitative and qualitative data is needed.

Keywords: Aerosols, Thermal plume, Ventilation, Reynolds-Averaged Navier Stokes (RANS), Standard-RNG-Realizable K-ϵ, SST K-ω Turbulence Model.

1 Introduction

To mitigate the transmission of airborne viruses, gaining a thorough understanding of the mechanisms of viral dispersion is crucial. Following the 2019 outbreak of the SARS-CoV-2 virus, numerous prevailing assumptions were debunked [1, 2]. One notable example is the World Health Organization's delayed recognition of the virus's airborne transmission potential. It was not until October 20, 2020, that the organization acknowledged that aerosols which are minuscule droplets, could transmit the virus, categorizing it among a select group of airborne infections [3]. Consequently, indoor air quality emerged as a critical concern across various sectors, including healthcare, education, and manufacturing, due to the heightened risk of transmitting airborne infectious diseases [2].

Aerosols are fine respiratory particles that are less than 5 microns in diameter that can remain suspended in the air for long periods and travel long distances (>2 m), making them a suitable potential source of infection in poorly ventilated indoor spaces [4]. Thereby, airflow is recognized as the primary medium influencing the transmission of airborne diseases, with progressing evidence and numerous cases of reoccurrence over the years [5]. The process of airborne aerosol particles moving through the air and settling on surfaces is termed aerosol dispersion, which plays a significant role in indoor air quality [6].

The crucial promptness in studying the dispersion of infectious aerosols in indoor environments, assessing the potential risks, and developing effective control measures is of pressing importance. Understanding the physics of aerosol diffusion in indoor environments can help identify high-risk areas and develop strategies to reduce exposure and prevent infection. Unfortunately, experimental methods for studying aerosol dispersion in indoor environments have limitations in terms of cost, time, and the ability to control variables precisely [2]. These limitations result in incomplete data that does not fully capture the underlying physical processes involved in aerosol dispersion. Hence, there is a necessity for a numerical method that is both highly precise and dependable.

To effectively study aerosol dispersion, Computational Fluid Dynamics (CFD), a powerful tool for studying fluid flow, has been widely applied to investigate aerosol dispersion in indoor environments [1]. In this paper, we present a computational performance of the Reynolds-averaged Navier-Stokes (RANS) equations with aerosol dispersion in a ventilated indoor environment using four (4) different CFD turbulence models; Standard, RNG, Realizable k-ϵ, and SST k-ω turbulence flow. Based on the inherent accuracy compromise reported with turbulence models, it is imperative to investigate the performance of these turbulence models. These Computational Fluid Dynamics turbulence models have been applied to study aerosol dispersion in ventilated indoor environments [1, 2, 7].

RANS simulation solves the time-averaged Navier-Stokes equations, which model the mean flow and averages the effects of the turbulence in shorter time scales. RANS is widely used for industrial applications and is relatively computationally efficient compared to LES and DNS, which requires high computational resources. However, RANS may not accurately capture unsteady and three-dimensional turbulent flow fields, which is essential in aerosol dispersion [8].

RANS computational investigation using turbulence models such as Standard-RNG-Realizable k-ϵ and SST k-ω turbulence flow can provide insights into the behaviour of aerosols in indoor environments [9]. The complex nature of indoor settings, including obstacles and varying ventilation systems, makes it challenging to accurately model and predict aerosols' behaviour [9].

These computational models provide a promising alternative to experimental methods. However, there are limitations associated with these computational methods, including the need for accurate boundary conditions, assumptions, and computational resources [4].

In addition, it has been reported [10, 11] that subtle metabolic processes can significantly influence aerosols under the influence of diffusion, and these underlying effects are most predominant indoors. For instance, the constant rising of airflows around the boundary layer of the human body due to persisting temperature gradients between the body surfaces and the ambient air is referred to as the human body thermal plume [12]. Also, the interaction between the airflow and the mucous membrane of the nasal cavity makes possible the process of heating and moisturizing the air [13], thereby resulting in high-temperature air. The effect of the thermal plume (as shown in Figure 1) is primarily understated in the transmission pattern of aerosols. Effectively capturing the behaviour of this thermal flow in RANS is also highly dependent on the turbulence model.

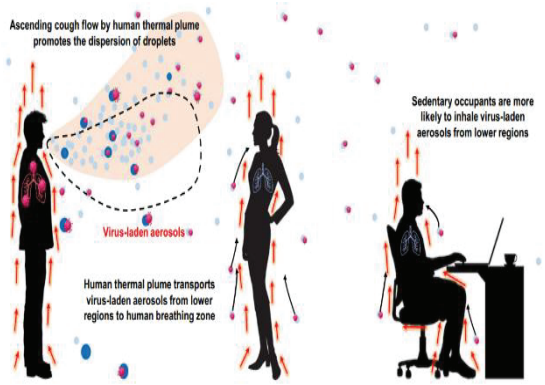

Fig. 1. Potential influences of the human thermal plume on the airborne transmission of COVID-19 [14].

Despite these understated effects and limitations, computational methods to study aerosol dispersion in indoor environments can provide valuable insights into the underlying physical processes. This study aims to qualitatively evaluate the accuracy and reliability of these computational RANS turbulence models in predicting aerosol diffusion patterns and thermal plumes in indoor environments.

2 Methods

Considering the importance of the effect of turbulence models for numerical simulations, four (4) different turbulence models were used to simulate the airborne dispersion from a single cough, namely; the Standard k-ϵ model, the Renormalization Group k-ϵ model (RNG), the Realizable group k-ϵ model and the Shear-Stress Transport (SST) k-ω model. For the sake of brevity, the equations are not repeated here. All the equations can be found in recent publications [15-18].

Numerical model

The human body is set up using a CAD-simplified human body of 1.77m in height. The simplified human body of area 1.72 m^2 is located at 0.5m in length, mid-width from the wall of a room of 3m (length) x 3m (width) x 3m (height), with air inlet and outlet on adjacent walls of the room as shown in Fig. 2. The boundary condition was set at inlet air supply velocity of $0.5ms^{-2}$. A constant room temperature of 20ºC was adopted. Moreover, to simulate the generated heat on the simplified human body, a constant body temperature of 37ºC was also assigned. The cough velocity with the exhaled aerosol particles is at $11.2ms^{-2}$ and the size distribution ranges from 0.3 to 30 micrometers in the computational ventilated room domain was tracked using the Lagrangian particle tracking approach for particle diffusion in the room. A reduced size distribution was chosen to specifically target smaller particles that remain suspended in the air for extended periods of time. The evaporation effect is not taken into consideration in this analysis.

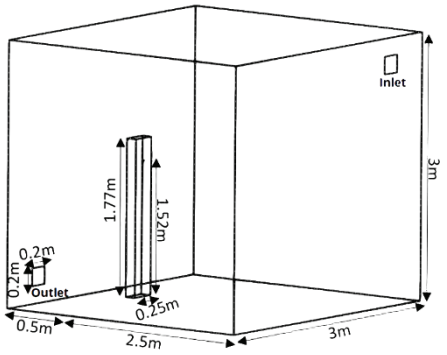

Fig. 2. The CAD geometry of the computational domain representing the room with a simplified human box.

The CFD tool ANSYS Fluent 2022 R2 was utilized, using the SIMPLE algorithm in the pressure and velocity coupling [19]. The no-slip boundary condition was assigned to all walls, and all the room walls were assumed to have adiabatic boundary conditions. A timestep size of 0.003s was uniformly utilized for all the steady-state simulations, correlating to a Courant number of 10.

Mesh details

This study adopted the mesh independence study procedure to guarantee the results' independence with grid resolutions for all the computational cases. Unstructured tetrahedral grids with ten (10) inflation layers were used for the setup. Four (4) grid sizes of 565,471, 756,432, 1,018,793, and 1,445,000 elements were numerically simulated and analyzed. The fine grid of 1,018,793 cells was selected to be sufficient for the computational calculation (Fig 3.).

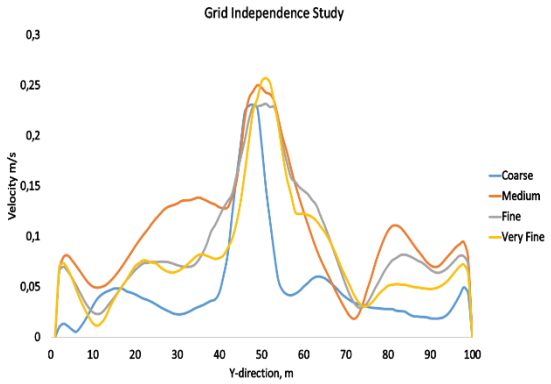

Fig. 3. Grid Independence study.

3 Results and Discussion

The background study on RANS turbulence modeling has provided an overview of four (4) turbulence models; Standard, RNG, Realizable k-ϵ, and SST k-ω. This discussion will focus on the implications and results of using these different models in aerosol particle dispersion and the advantages and limitations associated with each model. Table 1 shows the number of particles tracked by the various RANS turbulence models that were analyzed under the same boundary condition.

The Rosin Rammler function in ANSYS Fluent was utilized to control the aerosol size distribution.

Table 1. The total number of particles tracked.

Turbulence Models	Number of Particles tracked
Standard k-ϵ	3,200
RNG k-ϵ	17,152
Realizable k-ϵ	17,152
SST k-ω	17,152

The side-view dispersion patterns of aerosol particles at residence times 0.3s, 0.9s, 5.4s, and 10.2s for the different turbulence models are shown in Figures 4-7.

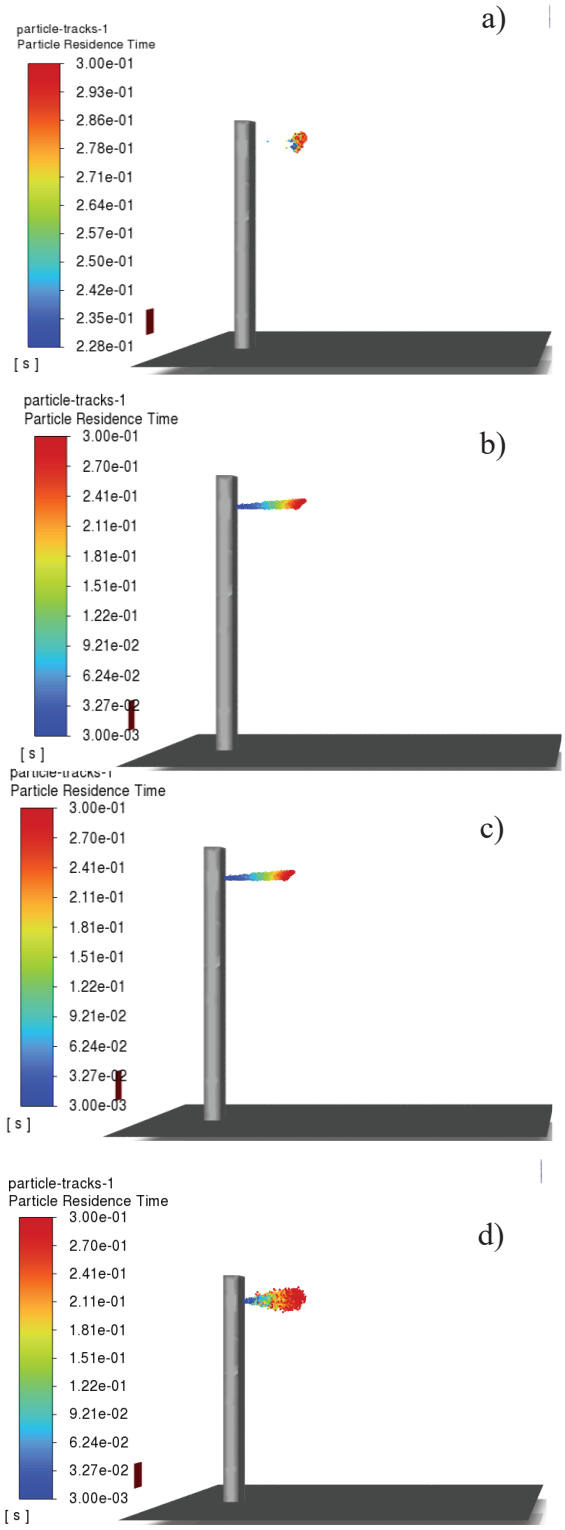

Fig. 4. Side-view dispersion patterns of aerosol particles at a residence time of 0.3s for turbulence models a) Standard b) RNG c) Realizable d) SST k-ω.

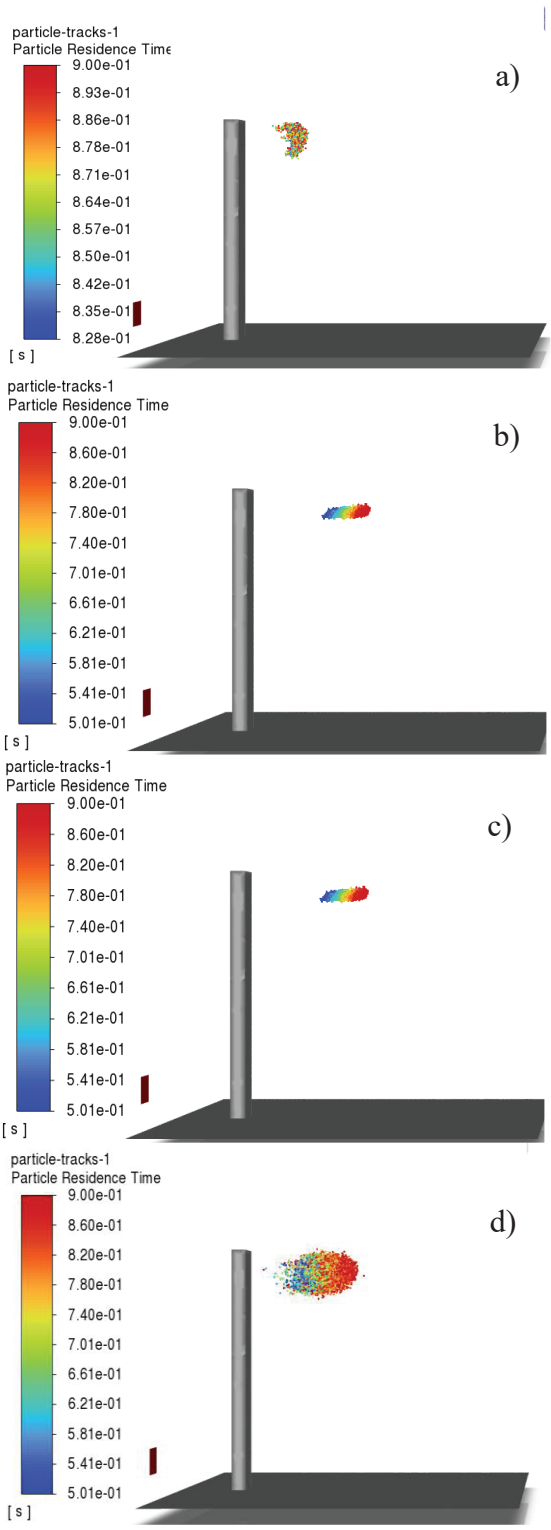

Fig. 5. Side-view dispersion patterns of aerosol particles at a residence time of 0.9s for turbulence models a) Standard b) RNG c) Realizable d) SST k-ω.

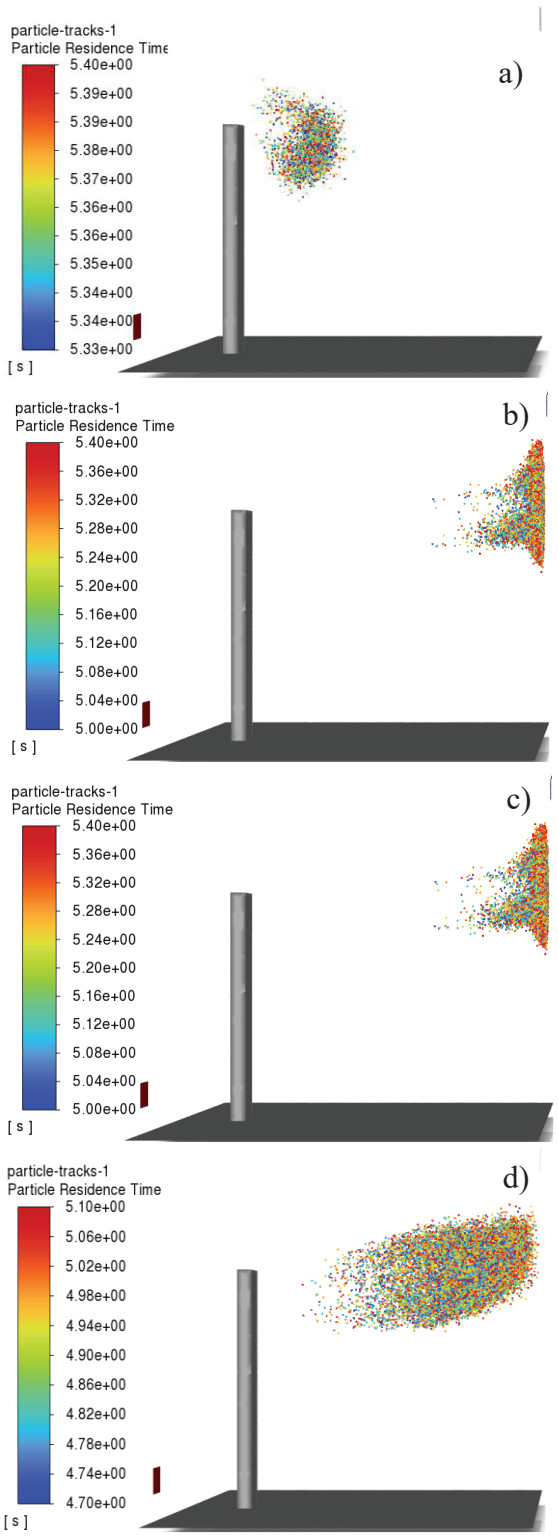

Fig. 6. Side-view dispersion patterns of aerosol particles at a residence time of 5.40 s for turbulence models a) Standard b) RNG c) Realizable d) SST k-ω.

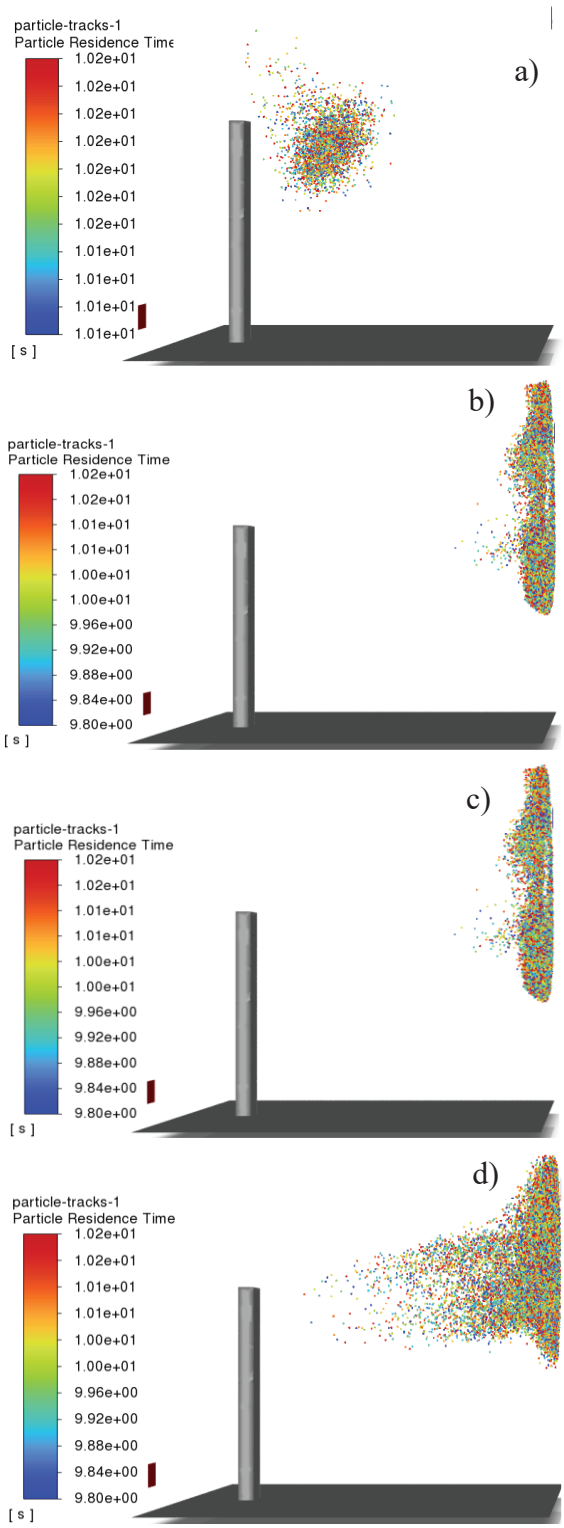

Fig. 7. Side-view dispersion patterns of aerosol particles at a residence time of 10.2s for turbulence models a) Standard b) RNG c) Realizable d) SST k-ω.

The aerosol dispersion pattern of the SST k-ω model is markedly different from those of the k-ϵ models, as shown in Fig.4-7. An explanation for this could be the SST k-ω model's incorporation of cross-diffusion term and the modification of turbulent viscosity to account for the transport of turbulent shear stress, leading to improved performance in capturing complex flow dynamics [10].

However, it may be more complex and computationally demanding than the other models, making it less suitable for some complex aerosol dispersion applications.

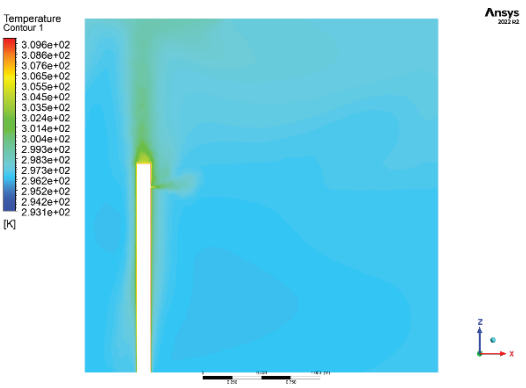

Fig. 8. Temperature contour for turbulence model Standard k-ϵ

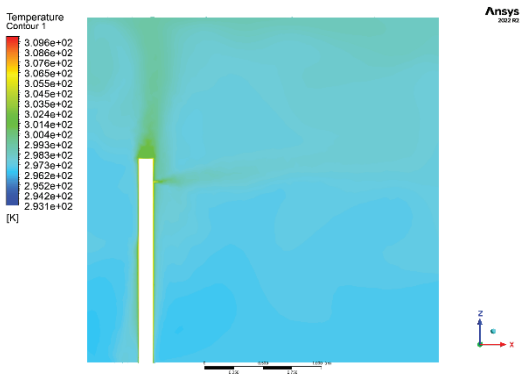

Fig. 9. Temperature contour for turbulence model RNG k-ϵ

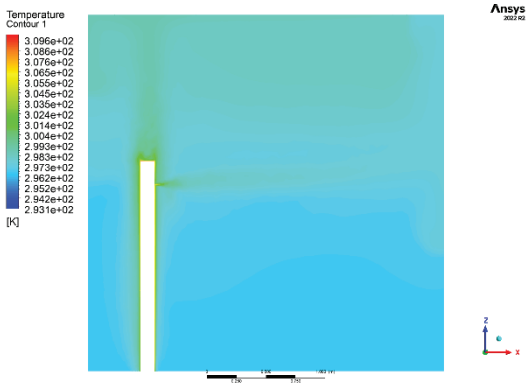

Fig. 10. Temperature contour for turbulence model Realizable k-ϵ

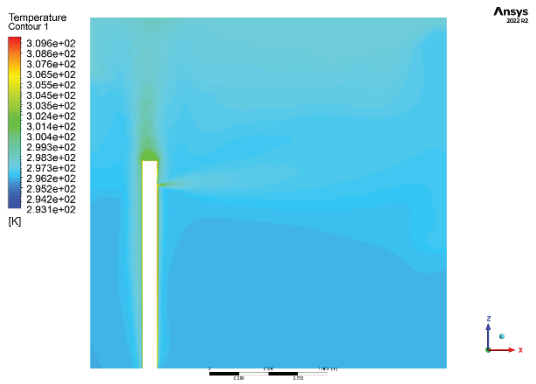

Fig. 11. Temperature contour for turbulence model SST k-ω

The contour plots shown in Fig.8-15 of the simulation study show that the dispersion pattern of the standard k-ϵ turbulence model may not be realistically compared to the actual airflow and particle behaviour in an indoor environment. This may be due to the model's inherent limitations in capturing complex flow dynamics. In addition, the simplified human body exhibited a thermal plume effect. The thermal plume influences the movement of respiratory droplets and airborne particles, especially in the near-human environment. The interaction between the thermal plume and cough-generated particles results in complex dispersion patterns (Figures 8-11), potentially affecting the transmission of airborne diseases. The standard k-ϵ model shows a stronger thermal plume effect around the simplified human body (Figure 8). This could also contribute to the aerosol particles' short travel distance and low aerosol particle concentration, as shown in Table 1.

On the other hand, the RNG and realizable k-ϵ models exhibit a high degree of similarity in their dispersion patterns, which may be attributed to their improved formulations that better account for the effects of turbulence, such as the consideration of the turbulent production term and the absence of singularities in the equations. This is also shown in the velocity contour results in Figures 13 and 14.

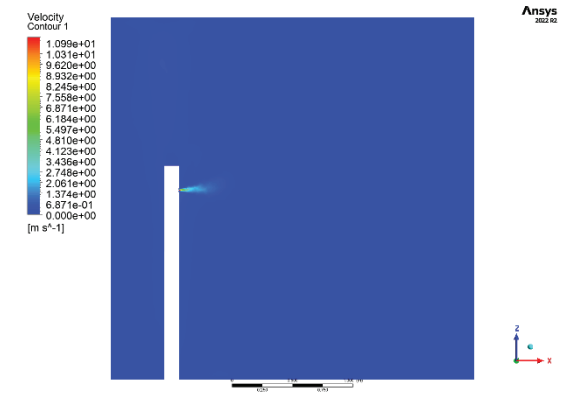

Fig. 12. Velocity contour for turbulence model Standard k-ϵ

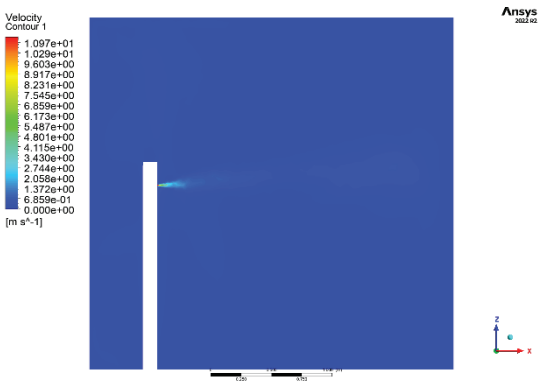

Fig. 13. Velocity contour for turbulence model RNG k-ϵ

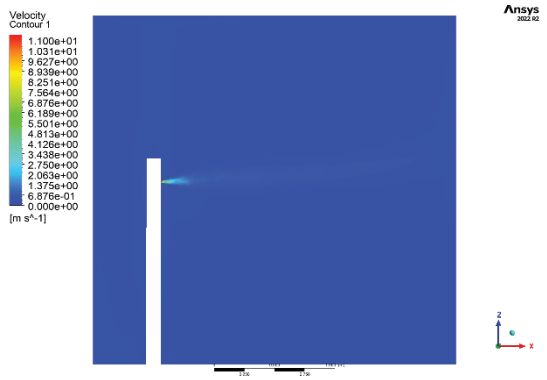

Fig. 14. Velocity contour for turbulence model Realizable k-ϵ

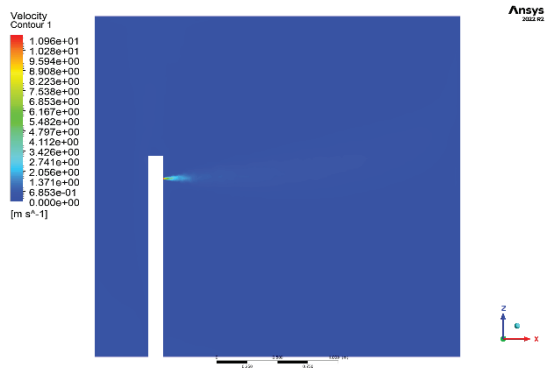

Fig. 15. Temperature contour for turbulence model SST k-ω

The velocity contour reveals similarities between the RNG and Realizable k-ε models (Figures 13 and 14) regarding their airflow patterns. Additionally, the SST k-ω model displays a faster decline in velocity compared to the RNG and Realizable k-ε models. However, with the exception of the standard k-ε turbulence model, the other three models demonstrate an oval-shaped pattern created by the cough dispersion, as seen in Figures 13-15.

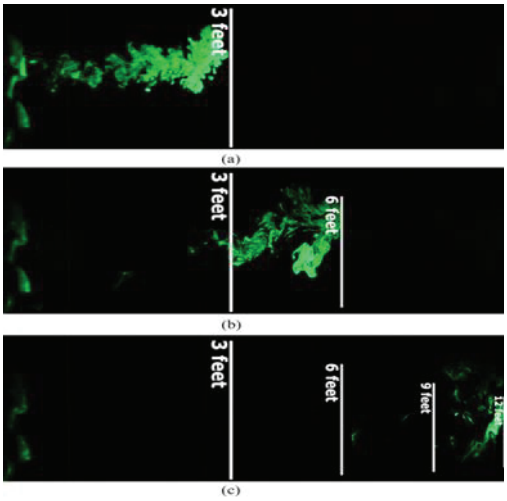

Fig. 16. An experimental emulated heavy cough jet for qualitative validation at (a) 2.3s, (b)11s, and (c) 53s [20].

Qualitatively comparing the results of the RANS model with available experimental data (Figure 16) from the literature makes it apparent that the standard k-ϵ turbulence model does not exhibit agreement.
In contrast, the RNG k-ϵ and realizable k-ϵ models show better agreement in dispersion pattern with experimental data, as they incorporate modifications that address some of the standard k-ϵ model's limitations. The SST k-ω model also demonstrated a good performance in capturing experimental aerosol dispersion patterns. Although the dispersion across the room is slower than RNG k-ϵ and realizable k-ϵ models.

However, it is essential to note that the experimental results [20] (Figure 16) provide more detailed information about the flow field, as they are based on direct observations of the physical system. RANS-based turbulence models, on the other hand, rely on approximations and simplifications to represent the complex nature of turbulent flows. While useful for many engineering applications, these models may not fully capture the intricacies of the aerosol flow behaviour, which can be observed more accurately in experimental studies.

4 Conclusion

The choice of an appropriate turbulence model is crucial for obtaining reliable CFD simulation results. This study investigated four (4) Computational Fluid Dynamics RANS turbulence models in predicting particle dispersion patterns in indoor environments, i.e., Standard-RNG, Realizable k-ϵ, and SST k-ω turbulence flow model.
The observed differences in the dispersion patterns can be attributed to the distinct formulations and assumptions underlying each turbulence model. The standard k-ϵ model appears to be less accurate in simulating particle dispersion, while the RNG and realizable k-ϵ models exhibit more significant similarities. The SST k-ω model, with its unique blending approach and additional terms, demonstrates a different dispersion pattern, which may better represent the actual behaviour of aerosol particles in various indoor environments.
On the other hand, the standard k-epsilon model's low number of tracked aerosol particles compared to other models could be due to its limited ability to model near-wall effects.
By comparing the results obtained from the four (4) RANS models with the experimental data presented in Figure 16, it becomes evident that the RANS results lack accuracy and detail. The inherent assumption of RANS, which involves time-averaging the flow and neglecting unsteady or transient effects, is demonstrated to be inadequate in accurately capturing the observed phenomena.
However, to determine the most suitable turbulence model for accurately representing cough flow and aerosol dispersion dynamics, it is necessary to conduct a thorough validation against both quantitative and qualitative data.

References

[1] S. Peng, Q. Chen, and E. Liu, "The role of computational fluid dynamics tools on investigation of pathogen transmission: Prevention and control," *Science of The Total Environment,* vol. 746, p. 142090, 2020.
[2] Z. T. Ai and A. K. Melikov, "Airborne spread of expiratory droplet nuclei between the occupants of indoor environments: A review," *Indoor air,* vol. 28, no. 4, pp. 500-524, 2018.
[3] D. Lewis, "Why the WHO took two years to say COVID is airborne," *Nature,* vol. 604, no. 7904, pp. 26-31, 2022.
[4] M. Jayaweera, H. Perera, B. Gunawardana, and J. Manatunge, "Transmission of COVID-19 virus by droplets and aerosols: A critical review on the unresolved dichotomy," *Environmental research,* vol. 188, p. 109819, 2020.
[5] S. Tang *et al.*, "Aerosol transmission of SARS-CoV-2? Evidence, prevention and control," *Environment international,* vol. 144, p. 106039, 2020.
[6] L. Morawska, "Droplet fate in indoor environments, or can we prevent the spread of infection?," in *Indoor Air 2005: Proceedings of the 10th International Conference on Indoor Air Quality and Climate*, 2005: Tsinghua University Press, pp. 9-23.
[7] S. Zhu, S. Kato, and J.-H. Yang, "Study on transport characteristics of saliva droplets produced by coughing in a calm indoor environment," *Building and environment,* vol. 41, no. 12, pp. 1691-1702, 2006.
[8] E. Nof, S. Bhardwaj, P. Koullapis, R. Bessler, S. Kassinos, and J. Sznitman, "In vitro–in silico correlation of three-dimensional turbulent flows in an idealized mouth-throat

model," *PLOS Computational Biology,* vol. 19, no. 3, p. e1010537, 2023.
[9] G. H. Downing *et al.*, "Computational and experimental study of aerosol dispersion in a ventilated room," *Aerosol Science and Technology,* vol. 57, no. 1, pp. 50-62, 2022.
[10] W. W. Nazaroff, "Indoor particle dynamics," *Indoor air,* vol. 14, no. Supplement 7, pp. 175-183, 2004.
[11] C. J. Weschler and W. W. Nazaroff, "Semivolatile organic compounds in indoor environments," *Atmospheric environment,* vol. 42, no. 40, pp. 9018-9040, 2008.
[12] S. Sun, J. Li, and J. Han, "How human thermal plume influences near-human transport of respiratory droplets and airborne particles: a review," *Environmental Chemistry Letters,* vol. 19, pp. 1971-1982, 2021.
[13] A. Issakhov, A. Mardieyeva, Y. Zhandaulet, and A. Abylkassymova, "Numerical study of air flow in the human respiratory system with rhinitis," *Case Studies in Thermal Engineering,* vol. 26, p. 101079, 2021.
[14] S. Sun, J. Li, and J. Han, "How human thermal plume influences near-human transport of respiratory droplets and airborne particles: a review," *Environmental Chemistry Letters,* vol. 19, no. 3, pp. 1971-1982, 2021.
[15] S. A. Holmes, A. Jouvray, and P. G. Tucker, "An assessment of a range of turbulence models when predicting room ventilation," in *Proceedings of Healthy Buildings*, 2000, vol. 2, pp. 401-406.
[16] V. Yakhot and S. A. Orszag, "Renormalization group analysis of turbulence. I. Basic theory," *Journal of scientific computing,* vol. 1, no. 1, pp. 3-51, 1986.
[17] T.-H. Shih, N.-S. Liu, and K.-H. Chen, "A non-linear k-epsilon model for turbulent shear flows," in *34th AIAA/ASME/SAE/ASEE Joint Propulsion Conference and Exhibit*, 1998, p. 3983.
[18] F. R. Menter, "Two-equation eddy-viscosity turbulence models for engineering applications," *AIAA journal,* vol. 32, no. 8, pp. 1598-1605, 1994.
[19] A. Fluent, "12.0 Theory Guide," *Ansys Inc,* vol. 5, no. 5, p. 15, 2009.
[20] S. Verma, M. Dhanak, and J. Frankenfield, "Visualizing the effectiveness of face masks in obstructing respiratory jets," *Physics of Fluids,* vol. 32, no. 6, p. 061708, 2020.